Reference: *Biol. Bull.* **174**: 303–318. (June, 1988)

Development and Larval Morphology of the Spiny Scallop, *Chlamys hastata*

CHRISTINE A. HODGSON[1] AND ROBERT D. BURKE

Department of Biology, University of Victoria, Victoria, British Columbia V8W 2Y2

Abstract. The early life history of *Chlamys hastata*, the spiny scallop, from spawning through metamorphosis to a benthic juvenile is described using light and electron microscopy. Newly released oocytes were about 70 μm in diameter and occasionally were surrounded by a 65 μm-thick jelly coat. A low envelope that is elevated at fertilization was observed in SEM preparations. Gastrulation results from both epiboly and invagination. Primary trochoblasts can be distinguished as two groups of ciliated cells surrounding the blastopore. The D-stage veliger developed by about 50 hours (12°C) and the planktotrophic larval stage is about 40 days in duration. Veliger larvae reached a maximum valve length of 240 μm. Provinculum length remained constant throughout larval life and a ligament may be present in the larval stage. An interlocking crown and groove feature on the larval denticles is described. There is a group of distinctive compound cilia situated at the mouth region that may function in particle sorting. Development of *C. hastata* is superficially similar to that of other species of pectinids. However, differences in details of larval morphology suggest there is greater variation in larval form and function than is generally assumed.

Introduction

Embryonic development and larval morphology of several species of lamellibranch has been described (see review by Wada, 1968; Andrews, 1979; Sastry, 1979; Verdonk *et al.*, 1983). Species that have been examined include *Ostrea edulis* (Waller, 1981; Cranfield, 1973a, 1973b; Hickman and Gruffydd, 1971), *Crassostrea virginica* (Elston, 1980), and *Mytilus edulis* (Lane and Nott, 1975; Bayne, 1971). However, there are only a few studies that provide details on larval organs in pectinids. Cragg and Nott (1977) examined ultrastructure of statocysts in *P. maximus* pediveligers and glands in the foot of *Pecten maximus* were examined by Gruffydd *et al.* (1975). As well, hinge morphology of *Chlamys varia* (LePennec, 1980), *C. distorta, C. opercularis,* and *P. maximus* (LePennec, 1978, from LePennec, 1980) has been described.

Chlamys hastata is found from the Gulf of Alaska to southern California at depths to 150 meters (Bernard, 1983). It is primarily dioecious, reaches sexual maturity at two years, and is thought to spawn annually during the summer months. Adults attain a maximum valve height of 8 cm and generally live about 4.5 years (Grau, 1959, B. MacDonald pers. com.). *C. hastata* supports a small fishery (68.5 tonnes in 1986; R. Harbo, pers. comm.) yet little is known about its early life history.

The objective of this report is to describe and document embryonic and larval development of *C. hastata,* from gamete release through metamorphosis to the benthic juvenile. Morphology of several larval organs, valves, velum, foot, and gill rudiment, is also described.

Materials and Methods

Larval culture

Adult *C. hastata* were collected between June and August by SCUBA diving near Wizard Rock in Barkley Sound, British Columbia, and kept in a darkened, 20 l tank for two to five weeks and supplied with a continuous flow of seawater (14–16°C). Three times daily, several liters of supplemental phytoplankton ($2–3 \times 10^6$ cells/ml) were added.

Scallops were taken from the holding tank for spawning, epifauna removed, and the sexes separated. Seawa-

Received 22 September 1987; accepted 25 March 1988.

[1] Present address: Department of Fisheries and Oceans, Pacific Biological Station, Nanaimo, British Columbia, V9R 5K6.

ter, irradiated by ultraviolet light, was dripped into the spawning buckets and the water warmed from 12°C to 18°C over a period of one to two hours. Males generally spawned after 20 to 60 minutes and females took up to three hours.

Gametes were collected and immediately washed with 0.8 μm glass-filtered seawater. The oocyte suspension was passed through a 253 μm screen to remove debris, and collected and rinsed on a 20 μm screen. The sperm suspension was passed through a 100 μm screen and added to the oocytes. After 6–10 min, fertilized oocytes were rinsed to remove excess sperm and transferred to 0.45 μm membrane-filtered seawater (FSW) (12°C). Water was changed twice during embryonic development and D-stage veliger larvae were transferred to 2 l vessels containing FSW (16°C) 50 mg/l streptomycin sulphate and 2 mg/l chloramphenicol. Larvae were fed phytoplankton daily ($1–4 \times 10^5$ cells/ml) and water changed every 2–3 days. Phytoplankton used for this study included *Nannochloris atomus, Pavlova lutheri, Isochrysis galbana, Thalassiosira weissflogii,* and *Dunaliella tertiolecta.*

Micrography

Larvae and post-larvae were photographed while swimming or crawling, or while contained within a small piece of Nitex mesh placed on a microscope slide. Occasionally, larvae were narcotized with isotonic $MgCl_2$ to observe larval structures.

For scanning electron microscopy (SEM), valves of larvae and juveniles at different stages were cleaned in distilled water for 30 min to remove soft tissues (Calloway and Turner, 1978) followed by immersing the valves in a 6% solution of sodium hypochlorite for approximately 10–15 min. Cleaned valves were stored in 70% ethanol until required for SEM (Lutz *et al.,* 1982). Valves were disarticulated by shaking vigorously in 6% sodium hypochlorite. Specimens were then rinsed in distilled water and mounted on double-sided sticky tape, sputter coated with gold, and viewed using a Jeol JSM-35 scanning electron microscope. Prior to photographing, each specimen was positioned so that four points along the shell margin, each at 90° intervals, were in exactly the same plane of focus to ensure accurate measurements (Lutz *et al.,* 1982).

Larvae and post-larvae at different stages were relaxed using 1:1 15% solution of $MgCl_2$ and seawater. Specimens were initially fixed for 1 h at room temperature in 2.5% gluteraldehyde, in 0.2 *M* phosphate buffer (Millonig, 1961) and 0.14 *M* NaCl (Cloney and Florey, 1968). Specimens were then rinsed in 0.2 *M* phosphate buffer containing 0.34 *M* NaCl, post-fixed 1 h at 7°C in 2% OsO_4 in 0.2 *M* phosphate buffer, and rinsed twice for 10 min in distilled water. Specimens were dehydrated in a graded series of ethanol and critical point dried using CO_2 as a transitional fluid. Specimens were mounted on stubs and gold coated.

For histological sections, specimens were relaxed and fixed as above. Following secondary fixation the specimens were decalcified in a 1:1 solution of 0.4% ascorbic acid and 0.34 *M* NaCl for 24–48 h (modified from Dietrich and Fontaine, 1975). After being rinsed in distilled water, dehydrated in a graded series of ethanol, and embedded in Epon (Luft, 1961), serial sections were cut, mounted, and stained with 1% azure II and 1% methylene blue in 1% sodium borax solution (Richardson *et al.,* 1960).

Results

Embryonic development

Spawned oocytes are about 70 μm in diameter. On two occasions, a 65-μm thick, translucent jelly coat surrounded each oocyte, making the total diameter about 200 μm (Fig. 1). The jelly coat was not evident using Koehler illumination but could be seen with phase contrast optics. Oocytes from most spawnings did not have a jelly coat (Fig. 2), and fertilization success and subsequent development of oocytes with or without a jelly coat was identical. Germinal vesicles appeared as a translucent region on the periphery of the oocyte.

Sperm of *C. hastata* remain active for at least 2 hours after release. Head and midpiece of sperm is about 4 μm long and tail is 40 μm long (Fig. 3). The conical sperm head is 1.25 μm wide at the base and tapers to 1 μm wide at the tip. A 1.25 μm long acrosome is situated at the tip of the sperm.

A fertilization envelope and underlying vitelline space are apparent using SEM (Fig. 3). The fertilization envelope is a thin sheet supported by cytoplasmic extensions of the oolemma. The vitelline space is 0.8–1.0 μm thick and the egg surface appears slightly pitted.

Polar body formation begins about 20 min after fertilization (12°C) (Fig. 4). First cleavage is meridional, unequal, and initiated 3 h after fertilization (Fig. 5). A deep cleavage furrow begins at the animal pole, the site of polar body release, and a large polar lobe forms at the vegetal pole. The polar lobe fuses with the CD blastomere before first cleavage is complete (Figs. 6, 7). Second cleavage is also meridional, perpendicular to the first cleavage plane and is complete by 3.75 h. A, B, and C blastomeres are of equivalent size and the D blastomere is slightly larger. Third cleavage is latitudinal and dexioplectic and unequal (Fig. 8). Within 15 h, the embryo has reached the morula stage, a non-motile ball of cells. Gastrulation occurs by epiboly and invagination is complete by 18 h (Figs. 9, 10). The micromeres extend over

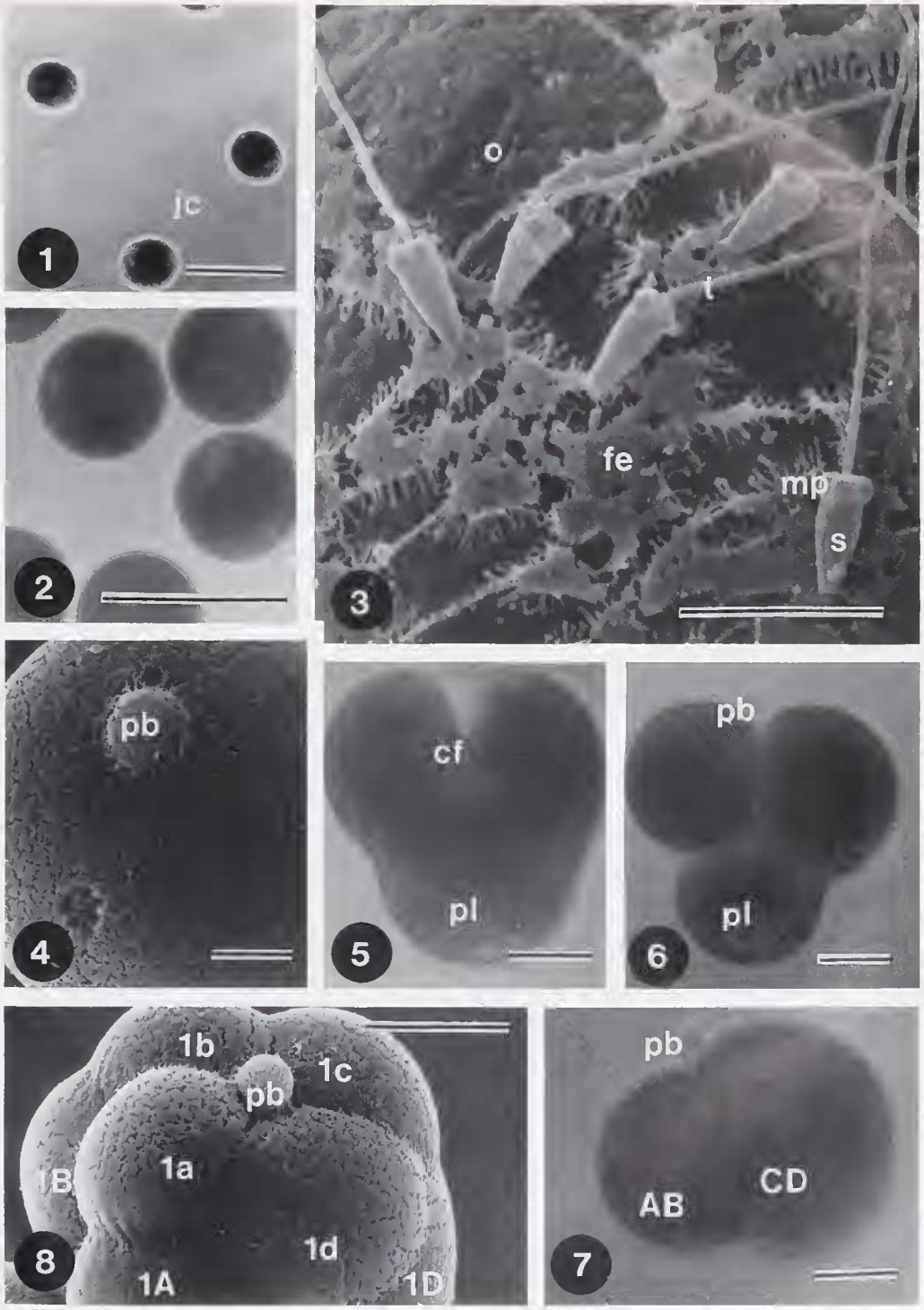

Figure 1. Primary oocytes with jelly coats (jc). Light micrograph (LM), phase contrast optics. Scale bar = 100 μm.

Figure 2. Primary oocytes lacking jelly coats. LM, bright field optics. Scale bar = 100 μm.

Figure 3. Scanning electron micrograph (SEM) of sperm cells (s) on surface of oocyte at fertilization. mp, midpiece; o, oolemma; t, tail; fe, fertilization envelope. Scale bar = 5 μm.

Figure 4. SEM of first polar body (pb) release. Scale bar = 10 μm.

Figures 5–7. First cleavage with polar lobe formation. Polar lobe (pl) forms at vegetal pole as cleavage furrow (cf) develops at animal pole. Polar lobe fuses with CD blastomere as cleavage becomes complete. LM, bright field optics. pb, polar body. Scale bar = 20 μm.

Figure 8. Third cleavage stage. Blastomeres labelled using nomenclature for spirally cleaving embryos. SEM. pb, polar body. Scale bar = 20 μm.

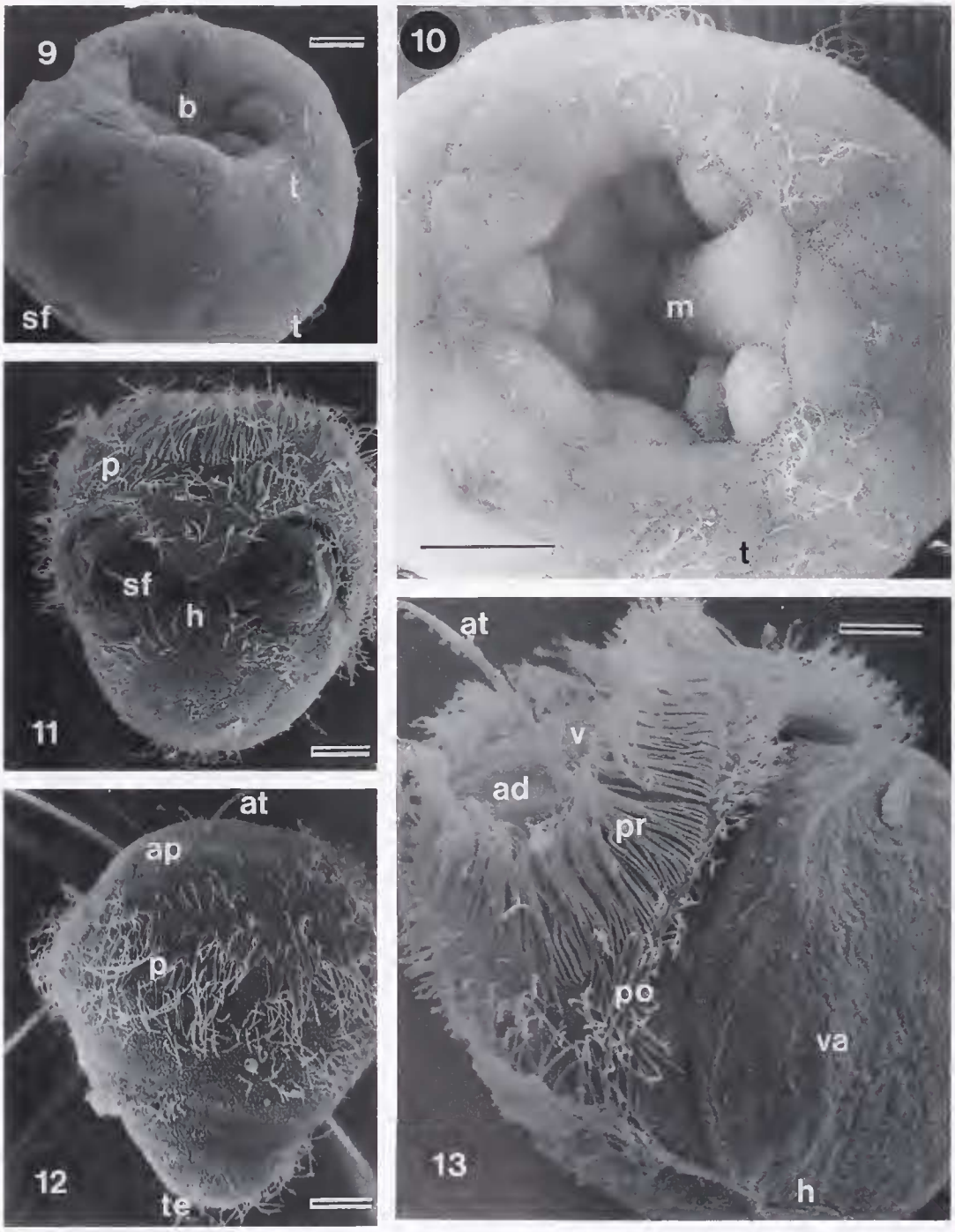

Figure 9. Blastopore (b) is initially a wide, shallow depression at vegetal pole. Ectodermal cells invaginate to form shell field (sf) on dorso-lateral surface. Two groups of ciliated cells, the primary trochoblasts, (t) are evident on perimeter of blastopore and on dorso-lateral surface. SEM.

Figure 10. Ventral view of blastopore. Invagination is deeper and perimeter of margin is narrower than in Figure 9. A single macromere (m) can be seen in the blastopore. SEM. t, primary trochoblasts.

Figure 11. Trochophore larva with developing shell field (sf) on dorsal surface. Shell secretion is initiated in two regions. SEM. h, future hinge; p, prototroch.

Figure 12. Trochophore larva. SEM. at, apical tuft; ap, apical plate; p, prototroch; te, telotroch.

Figure 13. Early D-stage larva, 45 h after fertilization, anterior view. Velum has two ciliated bands on outer margin. SEM. ad, apical disc; at, apical tuft; h, hinge region; pr, preoral band; po, postoral band; v, velum; va, valve. All scale bars = 10 μm.

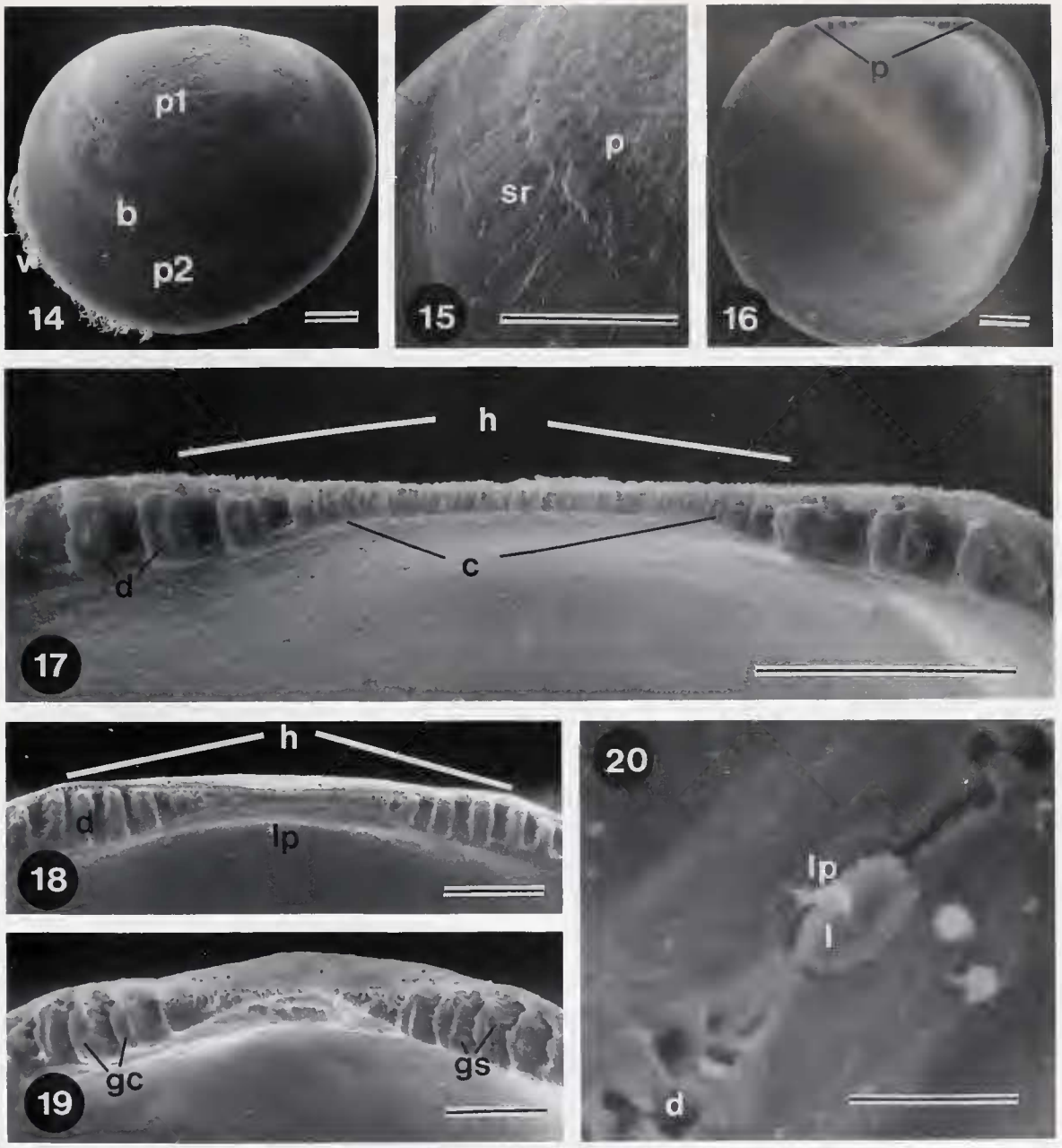

Figure 14. SEM of external surface of left valve of 15-day larva. b, prodissoconch I/II boundary; p1, prodissoconch I shell; p2, prodissoconch II shell; v, velar cilia.

Figure 15. Detail of Figure 14. SEM. p, punctate region and sr, stellate-radial region of prodissoconch I shell.

Figure 16. Internal surface of left valve of 15-day larva. SEM. p, provinculum.

Figure 17. Detail of Figure 16. SEM. d, denticles; c, cardinal region; h, hinge line.

Figure 18. Provinculum of 39-day larva. SEM. d, denticles; h, hinge line; lp, ligament pit.

Figure 19. Provinculum of 39-day larva. Note the crown of each denticle bears a groove (gc) and the sides bear transverse grooves (gs). SEM.

Figure 20. Hinge region of 39-day larva. SEM. d, denticles; l, ligament; lp, ligament pit. All scale bars = 20 μm.

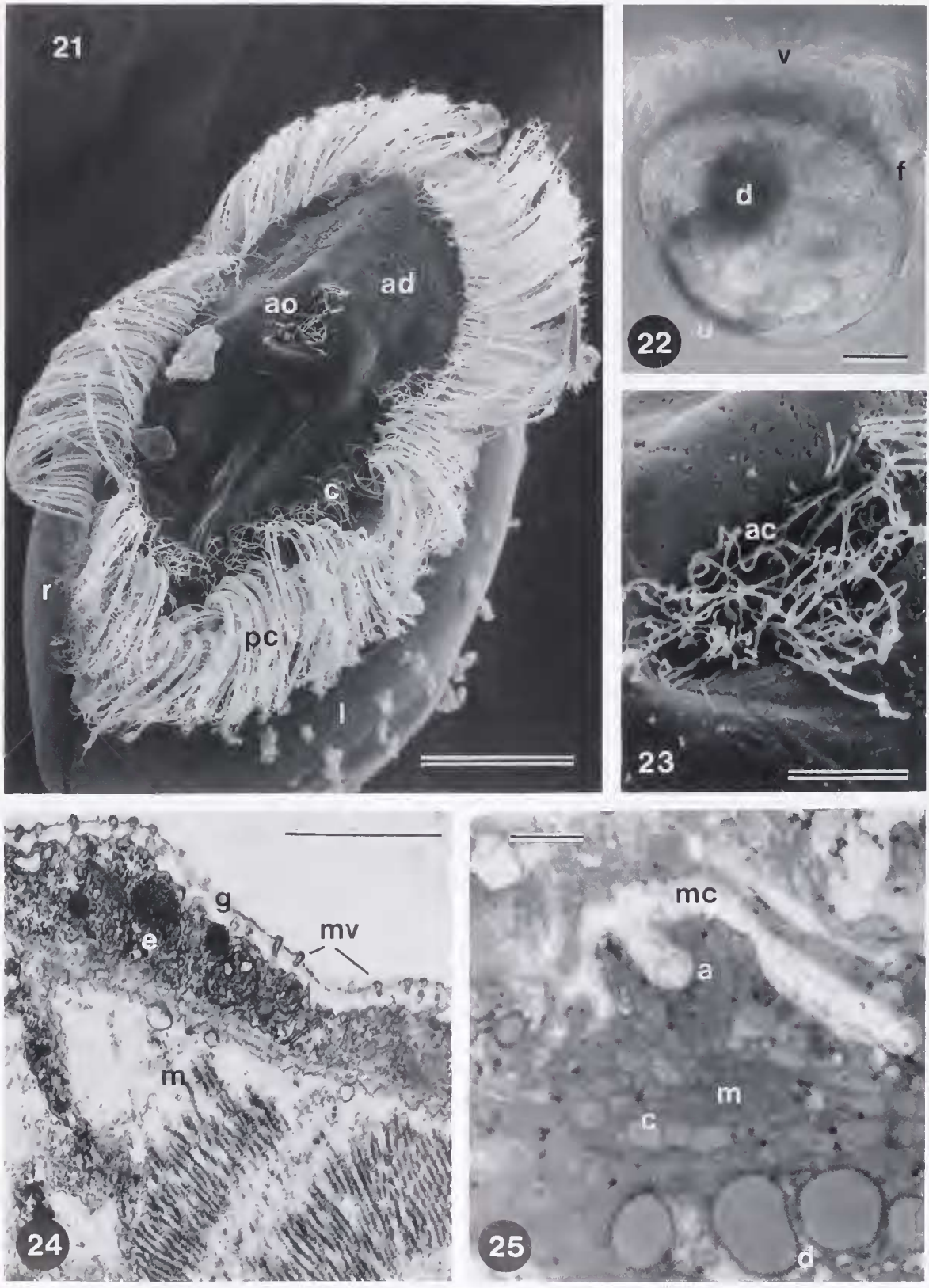

Figure 21. SEM of pediveliger larva with opened velum. A sparse band of simple cilia (c) is situated between the preoral cilia (pc) and the apical disc (ad). ao, apical organ; l, left valve; r, right valve; Scale bar = 50 μm.

and enclose the macromeres and then appear to sink into the blastopore. The blastopore is wide and shallow initially, but the opening becomes smaller as the invagination deepens. On the perimeter of the blastopore are two groups of 2–4 cells bearing sparse cilia, the primary trochoblasts (Fig. 10). Two other groups of primary trochoblasts girdle the embryo between the animal and vegetal poles (Fig. 9).

At 21 h, gastrulae hatch from their fertilization envelope and by 30 h trochophores swim near the surface of the water (Fig. 11, 12). The prototroch develops from the primary trochoblasts and encircles the mid-region of the trochophore as a 24 μm broad band of widely spaced, simple cilia. The apical tuft, a group of 8–10 fused cilia, is situated centrally on the apical plate, and projects forward 10–15 μm (Fig. 12). The posterior apex of the trochophore bears a small tuft of cilia, the telotroch, and the rest of the body wall is sparsely ciliated.

The shell field, located on the dorsal surface of the trochophore, begins secretion of the prodissoconch I shell in two regions (Fig. 9, 11). These two regions contact along the straight hinge line. Using Koehler illumination, larval valves are first apparent in 45-h-old larvae, but are not capable of closing completely (Fig. 13). Using cross polarized filters, birefringence was observed, indicating that the valves are calcified at this time. By 50 h the embryo has developed into a D-stage veliger. The valves are capable of closing and surrounding the entire larva. At this stage valve length is about 105 μm and valve height is 82 μm. The prototroch transforms into the velum of the veliger larva with two distinct rows of cilia, a row of 20-μm long compound cilia, the preoral band, and a row of shorter, simple cilia, the postoral band.

Larval morphology

Valves. The shell gland of the trochophore becomes the mantle of the D-stage larva and continues secretion of the valves. Two distinct types of shell are secreted, the prodissoconch I and prodissoconch II (Fig. 14). The prodissoconch I is comprised of two distinct regions, an area uniformly dimpled with shallow pits and a zone about 12–14 μm broad which is convex and radially striate (Fig. 14). Carriker and Palmer (1979) referred to this pattern as the punctate-stellate pattern. The prodissoconch II is smoother and is commarginally striate (after Waller, 1981).

The hinge region, or provinculum, of 15-day-old larvae consists of a narrow, smooth ridge along the hinge line with 3–4 small stout denticles at either end in a narrow, triangular depression (Fig. 16, 17). Development of the denticles at both ends is symmetrical. Mean hinge length in 15-day larvae is 75.3 ± 15.6 μm, and mean provinculum length is 100.5 ± 21.8 μm. (n = 4). In pediveligers, the ridge along the hinge line is thicker and five to six denticles are present at either end (Fig. 18). Provinculum length, or distance between outer margins of outside denticles, remains constant throughout larval development, whereas the distance between the inner margins of the inside denticles is less in 39-day-old larvae (28.1 ± 9.9 μm (n = 2) *versus* 41.3 ± 12.7 μm (n = 4) for 15 day larvae). This indicates that additional denticles are added to the inside of the initial three denticles. In pediveligers, denticles are more pronounced and slightly longer than those of younger larvae and have a columnar appearance. The crest of each denticle is slightly indented along the long axis such that there are two small ridges perpendicular to the hinge (Fig. 19). The anterior and posterior sides of the denticles bear curved ridges which are concave toward the hinge line.

A ligament pit is evident in larvae about 210 μm in valve length as a shallow depression immediately below the hinge line in the center (Fig. 18, 19). The ligament is broad (about 15 μm) and takes up almost one-half of the area between the denticles (Fig. 20).

Maximum valve length in *C. hastata* pediveligers is 240 μm (39 days after fertilization). Larvae held longer than 40 days did not show an increase in valve length or height.

Velum. The velum is the oval locomotory and feeding organ of the larva (Figs. 21, 22). When extended, the ciliated margins of the velum protrude beyond the anterior edges of the valves. When retracted, the velum is folded anterior-posteriorly and occupies the anterior half of the mantle cavity. Retraction is achieved by the striated anterior and posterior retractor muscles, which have sev-

Figure 22. Swimming pediveliger larva with foot (f) extended. LM, phase contrast optics. d, right digestive diverticulum; u, umbo; v, velum. Scale bar = 50 μm.

Figure 23. Detail of Figure 21. Note apical cilia (ac) emerging from apical organ. SEM. Scale bar = 10 μm.

Figure 24. TEM of velar disc epithelium. e, epithelial cell; g, glycocalyx; m, muscle cell; mv, microvilli. Scale bar = 10 μm.

Figure 25. Histological section of apical organ and cerebral ganglion in pediveliger larva with partially retracted velum. a, apical cells; c, cortex and m, medula of cerebral ganglion; d, digestive diverticulum; mc, mantle cavity. Scale bar = 10 μm.

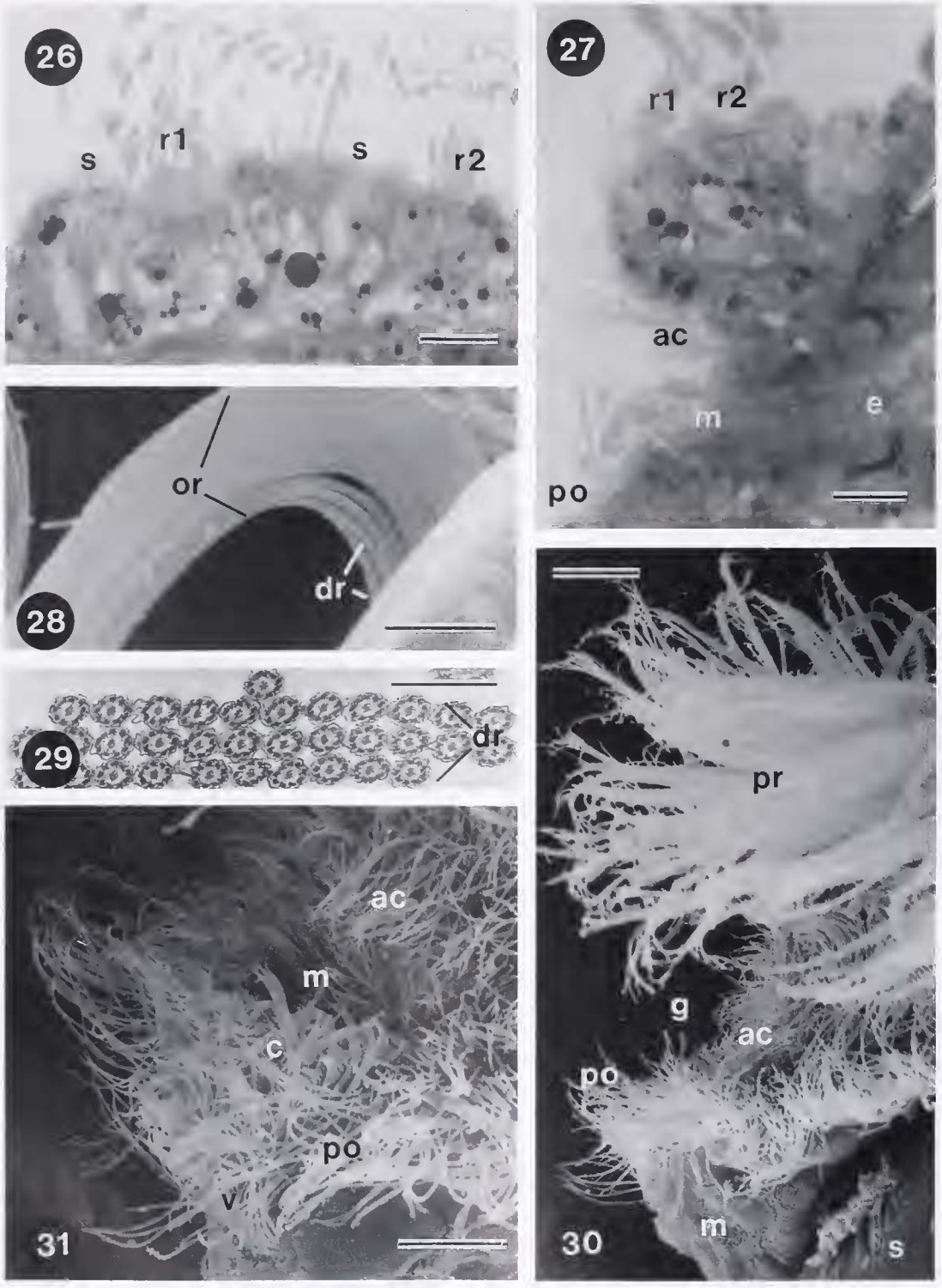

Figure 26. Tangential histological section of preoral band of velar margin. The preoral band consists of two rows of compound cilia (r1, r2) with secretory cells (s) situated between two rows and between the preoral and adoral ciliary bands. Scale bar = 10 μm.

Figure 27. Histological cross-section through ciliated bands on velar margin at the mouth region (m). ac, adoral cilia; e, esophagus; po, postoral cilia; r1, r2, double row of compound cilia of preoral band. Scale bar = 10 μm.

Figure 28. SEM of compound cilia of preoral band showing long orthoplectic rows (or) and short diaplectic rows (dr). Scale bar = 2 μm.

eral insertions on the epithelium of the velum along the anterior-posterior axis.

The apical plate of the trochophore remains as the central portion of the velum or apical disc. The apical tuft of the trochophore persists for 2–3 days in D-stage veligers. In older larvae this region becomes the apical pit, a small, deep invagination located in the center of the apical disc. The apical pit is oval in shape, approximately 6–8 μm wide, 20 μm long, and 10 μm deep (Fig. 23). Numerous fine, simple cilia originate from the apical pit and project a short distance beyond the rim of the pit. The epithelium of the apical disc is comprised of simple squamous to cuboidal cells that have a thick glycocalyx and numerous microvilli on their apical surfaces (Fig. 24). Cells of the apical pit are columnar, approximately 7 μm high, with apical nuclei. Directly underlying these cells is the cerebral ganglion (Fig. 25).

On the outer margin of the velum of D-stage veligers, compound cilia of the preoral band are arranged in a single row, and each compound cilium consists of two or three cilia adherent throughout their length (Fig. 13). In older larvae the preoral band consists of two rows of compound cilia (Figs. 26, 27). Each compound cilium is arranged in 6–15 orthoplectic rows and 2–6 diaplectic rows of cilia (Fig. 28, 29). Cilia comprising each compound cilium fit closely together along most of their length (Fig. 30). Cilia of the postoral band are simple and short (8 μm) and are arranged in one or two closely spaced rows (Figs. 27, 30). A third band of cilia between these two bands, the adoral band, is approximately 24 μm wide and the cilia are 8 μm long (Figs. 27, 30). A fourth, poorly defined band of 17 μm long simple cilia is situated between the apical plate and the preoral band (Fig. 21).

On the ventral surface of the velum the postoral band extends posteriorly and forms a V-shaped ventral lip, called the postoral tuft by Waller (1981) (Fig. 31). The mouth is situated anterior to the ventral lip, between the postoral and adoral cilia. Several short, broad compound cilia are located immediately ventral to the mouth. Each compound cilium consists of cilia not less than 8 μm in length arranged in a row of seven to nine cilia. The compound cilia are interspersed among the simple cilia of the postoral band.

In cross section, the outer margin of the velum is bilobed with the preoral and postoral bands at the apex of either lobe and the adoral band in a shallow trough between them (Figs. 27, 30). Cells of the ciliated bands are more columnar than other epithelial cells (Figs. 26, 27). Cells of the preoral band have large vacuoles in the basal region of each cell. Between the two rows of preoral cilia, and between the preoral and adoral bands, there are several secretory cells with large granules in their apical region (Figs. 26, 27).

Foot. The foot is first apparent in 15-day-old larvae as a small ciliated rudiment in the posterior-ventral region between the mouth and anus. This rudiment, the prepodium, forms the metapodium of the foot. About 28 days after fertilization the propodium develops rapidly from the anterior portion of the prepodium. By 34 days the foot is functional and larvae are often observed crawling on the substrate or swimming with the foot extended (Fig. 22). The foot is bilaterally symmetrical, about 110 μm long and 53 μm wide with a distinct toe and heel (Fig. 32). Lateral and dorsal surfaces of the foot are sparsely ciliated (Fig. 33). The ventral surface is covered with long (8–24 μm), simple cilia (Fig. 32) and has a byssal groove, 48 μm long, extending along the midline of the longitudinal axis. At the posterior-most region of the heel is a tuft of cilia (Fig. 32).

The primary byssus gland stains dark blue with Richardson's stain and is situated in the posterio-dorsal region of the foot, immediately posterior to the pedal ganglion (Fig. 34). Ventral to the primary byssus gland is an open, ciliated region—the lateral pouch—with two byssal ducts that pass ventrally to the sole of the foot (Fig. 34). Each duct is densely ciliated and lined with several secretory cells which probably also pass secretion granules into the duct. The ducts open at the posterior region of the byssal groove on the sole of the foot (Fig. 32).

When crawling, both ciliary and muscular action aid in forward movement of the foot along the substrate. The remainder of the larval body is dragged along the substrate, behind the foot, with the hinge region posteriormost; the body is periodically moved forward by sharp contraction of the pedal retractor muscles. The tip of the foot occasionally lifts off the substrate or moves laterally in a swaying motion during forward movement, giving the impression of a sensory function. The velum is extended while crawling and probably aids in the forward movement of the larva. Periodically, the larva will lift off

Figure 29. TEM of cross-section of a single compound cilium of preoral band showing arrangement of cilia within a compound cilium. dr, diaplectic row. Scale bar = 0.5 μm.

Figure 30. Cross-sectional view of ciliated bands on velar margin. SEM. ac, adoral cilia; g, food groove; m, mantle tissue; pr, preoral cilia; po, postoral cilia; s, shell. Scale bar = 10 μm.

Figure 31. Mouth region at posterior edge of velar margin. The mouth (m) is situated between the adoral (ac) and postoral (po) ciliary bands. Several short, compound cilia (c) are located just ventral to mouth. SEM. v, ventral lip. Scale bar = 10 μm.

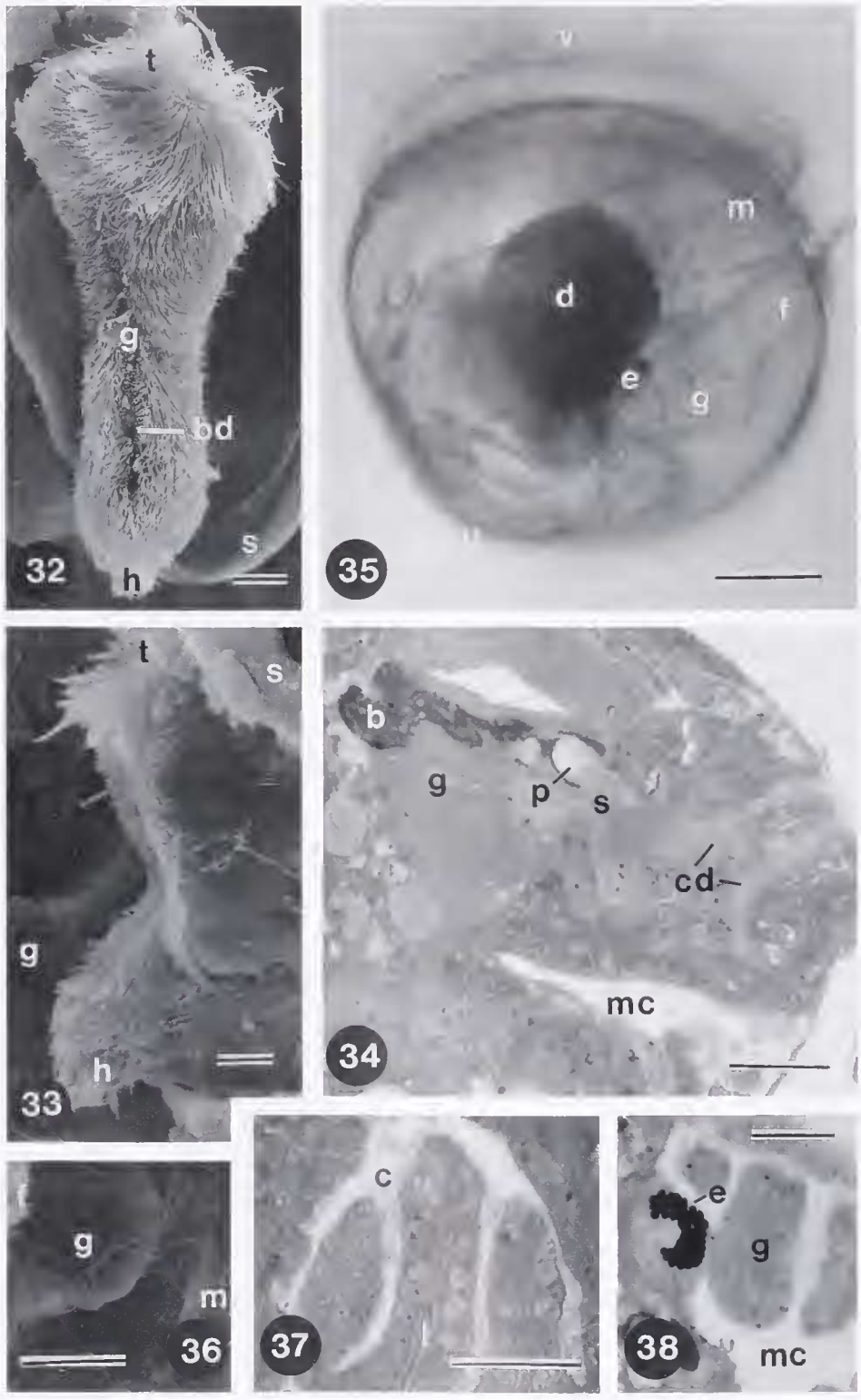

Figure 32. SEM of ventral surface of foot of pediveliger larva. Note dense ciliation on sole of foot with byssal groove (g) running medially from toe (t) to heel (h). SEM. bd, region of byssal duct; s, shell. Scale bar = 10 μm.

Figure 33. Lateral view of foot of pediveliger larva. Note dense cilia on sole of foot and only sparse cilia on lateral surface. SEM. g, gill rudiment; h, heel; s, shell; t, toe. Scale bar = 10 μm.

the substrate and swim, leaving the foot extended (Fig. 22).

Gill rudiment. Gill rudiments are first visible in larvae about 26 days old. On either side of the foot, a ridge of tissue—the gill plate—extends from the mantle into the mantle cavity. From each gill plate three small lobes of tissue, the primary gill filaments, develop (Fig. 35). By 32 days each rudiment is about 22 μm long and is sparsely ciliated with a single row of simple cilia along the apical margin that beat inward with an anteriorly directed metachronal wave (Fig. 36).

The primary filaments consist of a simple cuboidal epithelium with large vacuoles filled with granules (Fig. 37). Each filament has a narrow ciliated lumen. No cellular or ciliary connection between gill filaments on opposing sides of the mantle cavity was observed.

The larval eyes are first visible in larvae about 24 days old (Fig. 35) and are located on the anterior aspect of each gill bar. The larval eye consists of two cells, one with darkly staining granules arranged in a cup shape oriented anteriorly, and the other situated within the cup shape (Fig. 38).

Post-larval morphology

Length of larval development is about 40 days. At the pediveliger stage, valve length is about 240 μm; the foot is functional, and the gill rudiments are distinct. At metamorphosis, *C. hastata* transforms from a swimming pediveliger to a crawling, benthic post-larva within 24–48 hours. The internal organs of the larva undergo a 90° counter-clockwise rotation. The velum is histolized and the mouth moves from a ventral to an anteriodorsal position. As well, the foot moves anteriorly. Approximately 24 hours after metamorphosis has been initiated the foot is in a ventral position (Fig. 43), and by 48 hours after metamorphosis the foot is in an anterior position and individuals can crawl on the substrate with the hinge pointing in the direction of movement. The gill rudiments undergo rapid histogenesis to develop into the adult gills. With the forward rotation of the mouth region and foot, the gill filaments come to occupy the posterior region of the mantle cavity.

Once metamorphosis is complete, the mantle folds begin secretion of the dissoconch shell. Secretion of the left valve is initiated first and is visible in juveniles two days after metamorphosis (Fig. 39). The left valve has strong radial striations and formation of the anterior auricle is evident in early juveniles (Fig. 40). The right valve is smooth and a byssal notch is evident by three or four days after metamorphosis (Fig. 41). The dissoconch shell is secreted with little convexity and growth proceeds more rapidly in the direction of shell height than shell length.

The provinculum is thicker and the ligament pit is larger (19 ± 1.8 μm, n = 6) and more pronounced in 14 day old juveniles (Fig. 42). No further denticles are added after metamorphosis and larval denticles are gradually lost by overgrowth of juvenile shell. A ligament scar is evident at the region of the ligament pit, providing an increased surface to which the ligament attaches (Fig. 42).

At metamorphosis, the primary gill filaments lengthen and more are added (Fig. 43). By 2–3 days after metamorphosis, the single row of simple cilia present in the larval gill rudiments becomes the lateral ciliated band of the adult gill lamellae (Fig. 44). Length of gill lamellae is about 28 μm at this time. Another band of cilia, the frontal cilia, is just beginning to develop by 2–3 days and is clearly visible in 12 day old juveniles (Fig. 45).

Discussion

A jelly coat surrounding newly released oocytes has not been reported in pectinid species other than *C. hastata,* however, jelly coats do surround eggs of *Patinopecten yessoensis* and *Crassadoma gigantea* (CAH, unpub. obs.). The presence of the jelly coat may be common among pectinid species but since it is translucent and difficult to observe using Koehler illumination, it is possible that it has not been noticed by other authors.

Evidence from this study suggests that gastrulation oc-

Figure 34. Histological section of foot region. Secretions (s) of primary byssus gland (b) are deposited into the lateral pouch (p) which leads into two ciliated ducts (cd). g, pedal ganglion; mc, mantle cavity. Scale bar = 10 μm.

Figure 35. Light micrograph of swimming pediveliger, 40 days after fertilization, with toe of foot (f) extended. LM, bright field optics. e, eyespot; d, right digestive diverticulum; g, right gill rudiment; m, mouth; u, umbo; v, velum. Scale bar = 50 μm.

Figure 36. SEM of anterior-most primary gill filament (g) from right gill plate of a pediveliger larva. Note the single row of cilia. f, foot; m, mantle. Scale bar = 10 μm.

Figure 37. Longitudinal histological section through primary gill filaments. c, cilia; l, lumen. Scale bar = 10 μm.

Figure 38. Histological section through primary gill filaments (g) and eyespot (e) of 33-day-old larva. Dense, pigmented granules are deposited in the shape of a cup within a single cell. mc, mantle cavity. Scale bar = 10 μm.

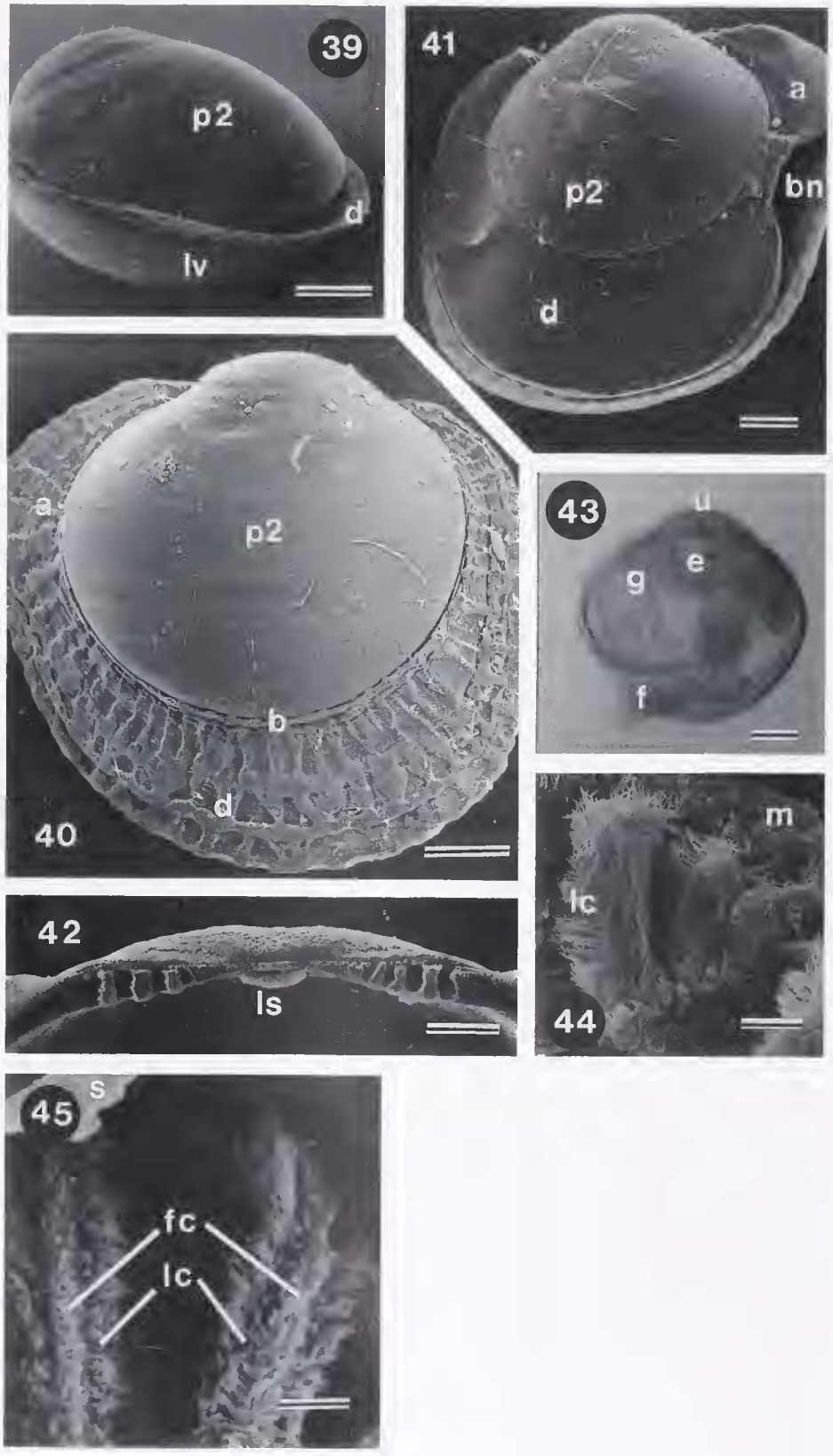

Figure 39. External view of postlarva, two days after metamorphosis, viewed from posterior region. Note dissoconch shell (d) on left valve (lv). SEM. p2, prodissoconch shell. Scale bar = 50 μm.

curs by both epiboly and invagination (Figs. 9, 10). This agrees with observations by Raven (1958) of *O. edulis* embryos. Other lamellibranchs in which this form of gastrulation has been observed include *Ensis, M. edulis* and *Teredo* (Verdonk and Biggelaar, 1983).

The two groups of cells located near the perimeter of the blastopore are probably two groups of the quartet of ciliated cells called the primary trochoblasts. Ultimately, they form the prototroch of the trochophore and ciliated bands of the velum in the veliger stage. These are generally described as originating from four points around the equatorial region of the embryo whereas the blastopore invaginates at the vegetal pole. However, the blastopore is displaced anteriorly during development and the pretrochal region is shifted forward, owing to considerable growth of the dorsal region, and the main axis of the embryo becomes bent such that the blastopore becomes situated in front of the prototroch (Verdonk and Biggelaar, 1983). Since the mouth is situated just below the prototroch, and ciliated bands of the velum, the location of the primary trochoblasts near the blastopore suggests that the blastopore becomes the future mouth.

The prodissoconch I shell of *C. hastata* bears the punctate-stellate pattern as first described by Ansell (1961). In published micrographs of *C. virginica* (Carriker and Palmer, 1979), the punctate region is about 30 μm in diameter, and in *O. edulis* (Waller, 1981) the region is ovoid, about 30 $\times$ 50 μm. Carriker and Palmer (1979) suggested that this region probably overlies the embryonic shell gland. However, in *C. hastata* the punctate pattern covers an area of about 40 $\times$ 80 μm (Fig. 14), about twice the size of the region of *O. edulis* or *C. virginica*. If indeed the punctate region represented the area of the embryonic shell gland, then the shell gland of *C. hastata* should be twice the size of shell glands of *O. edulis* and *C. virginica*.

The stellate-radial zone presumably represents the region where shell secretion is taken over by the mantle folds (Carriker and Palmer, 1979; Waller, 1981). Waller (1981) suggested that the transition from shell gland secretion to mantle secretion was gradual and occurred long before the prodissoconch I/II boundary in *O. edulis*. In his micrographs, it is apparent that the stellate-radial zone ends long before the prodissoconch I/II boundary and therefore his argument for the prodissoconch I/II boundary simply representing the first time of closure deserves consideration. The stellate-radial zone ends before the prodissoconch I/II boundary in *C. hastata* supporting Waller's hypothesis.

Other pectinids examined for larval hinge morphology are *P. maximus, C. varia, C. distorta* and *C. opercularis* (LePennec, 1980). Shell shape and hinge morphology of *C. hastata* larvae is similar to these species. All pectinids have hinge teeth which are symmetrical at each end with a thin cardinal ridge between which lacks cardinal teeth. *C. hastata* may have up to five or six denticles at each end by the time of metamorphosis whereas LePennec (1980) noted only three denticles in other pectinids. No further denticles were added after metamorphosis in *C. hastata*, which is similar to observations in other pectinids, except in *C. opercularis* which add one or two more denticles after metamorphosis.

In *C. hastata* larvae provinculum length remains constant throughout larval life. This contradicts the findings of Lutz and Hidu (1979) who examined provinculum lengths of *M. edulis* and *Modiolus modiolus* valves. They found that provinculum length increased with valve length and valve height by a linear relationship. The characteristic of a constant provinculum length, combined with hinge structure and valve dimensions, may be of assistance in distinguishing *C. hastata* larvae from other closely related species.

A common characteristic of bivalve larval denticles is the transverse ridges on the sides. *O. edulis* (Waller, 1981), *C. virginica* (Carriker and Palmer, 1979), *C. gigas* (Waller, 1981), *M. edulis* and *M. modiolus* (Lutz and Hidu, 1979), as well as *C. hastata* have transverse ridges. Lutz and Hidu (1979) suggested that the ridges reduce shear between the valves. A groove on the crown of each denticle of *C. hastata* corresponds to a small rise or bump located between each denticle of the opposing valve. No mention of these structures has been made in

---

Figure 40. External view of left valve of 12 day old juvenile. SEM. a, anterior auricle; d, dissoconch shell; b, prodissoconch II/dissoconch boundary; p2, prodissoconch II shell. Scale bar = 50 μm.

Figure 41. External view of right valve of 12 day old juvenile. Right valve is overlapped by larger left valve. Note distinct byssal notch (bn). SEM. a, anterior auricle; d, dissoconch shell; p2, prodissoconch II shell. Scale bar = 50 μm.

Figure 42. Proviniculum of 12 day old juvenile. SEM. ls, ligament scar. Scale bar = 20 μm.

Figure 43. Light micrograph of postlarva, one day after metamorphosis. Foot (f) is oriented ventrally and is very flexible (toe of foot is actually pointing posteriorly). Gill lamellae (g) occupy the posterior half of mantle cavity. LM, phase contrast optics. e, eyespot; u, umbo. Scale bar = 50 μm.

Figure 44. Proximal view of left gill lamellae of 4 day old juvenile. Note dense row of lateral cilia (lc) on 2 of the gill filaments. SEM. m, mantle tissue. Scale bar = 10 μm.

Figure 45. Distal view of gill lamellae of 12 day old juvenile. SEM. fc, frontal cilia; lc, lateral cilia; s, shell. Scale bar = 10 μm.

previous literature, and of the published scanning electron micrographs of larval valves in the literature, only *M. edulis* (Lutz and Hidu, 1979; see plate II, Figure A) also has a groove on the crown on each denticle. This crown and groove feature may further assist in the interlocking nature between opposing valves.

Neither the larval ligament nor the ligament pit was observed in other larval pectinids investigated (LePennec, 1980). Lutz and Hidu (1979) suggested the ligament is a post-larval feature, observed only after metamorphosis has been initiated. Larval valves of *C. hastata* capable of metamorphosing (39 days old at 16°C) had a ligament pit. The ligament pit may appear among larvae which are ready to metamorphose and not only in post-larvae.

Dissoconch shell of *C. hastata* is visibly different from, and is secreted at a faster rate than, prodissoconch II shell. These differences probably reflect the differences in the composition of the two types of shell. Prodissoconch I shell is entirely aragonitic (Stenzel, 1964) whereas dissoconch shell is entirely calcitic (Taylor *et al.*, 1969).

Among *C. hastata* post-larvae, the left valve is always slightly larger than the right valve. Even 12 days after metamorphosis, the right valve is about 12 μm smaller than the left valve. Secretion of the dissoconch left valve is initiated before secretion of the right valve and this may lead to the difference in size of the valves. This overlap of the left valve over the right valve has not been reported for other lamellibranch post-larvae.

The bilobe configuration of the outer margin of the velum was first noted by Elston (1980) in *C. virginica* larvae. Bivalve larvae probably feed by the opposed ciliated band method (Strathmann *et al.*, 1972; Strathmann and Leise, 1979) and this configuration may help keep particles in the food groove. According to the opposed ciliated band theory, the adoral cilia are responsible for transporting collected particles toward the mouth region, and the trough shape of the velar margin may assist in retaining particles in the region of the adoral cilia by creating a sunken channel in which the particles travel.

Secretory cells among the velar cilia have not been described previously, although other authors have either observed or assumed that mucus is involved in collection of particles (Yonge, 1926; Erdmann, 1935; Strathmann *et al.*, 1972; Waller, 1981). The mechanism by which veliger larvae are believed to capture food particles is direct interception of particles by the preoral cilia (Rubenstein and Koehl, 1977; Strathmann and Leise, 1979). Strathmann and Leise (1979) proposed that preoral cilia overtake particles in the latter part of the effective stroke and weakly adhere to them, pushing them faster than water. At the size and speed of ciliary movements involved in particle capture, viscous forces would dominate inertial forces (Vogel, 1981). Thus, at low Reynold's numbers the adhesion of small particles to rapidly moving cilia would probably not require an adhesive such as mucus. Rather than being involved in actual particle capture, materials released from the secretory cells instead may function in binding food particles, once already captured, into a string that travels along the adoral band, thus further ensuring the retention of food particles.

In *C. hastata*, the postoral band is comprised of simple cilia rather than compound cilia as observed in *O. edulis* (Erdmann, 1935; Waller, 1981). Since postoral cilia have been examined only in these two species it is difficult to generalize on the form of the postoral band among bivalve veligers. Whether the cilia are compound or simple may reflect on their role or efficiency in particle capture.

Compound cilia situated at the mouth region have not been previously described. Owing to their shape and location within the postoral band, we suggest their effective stroke is upward, toward the mouth, and therefore they are arranged in a single diaplectic row. Compound cilia arranged in row perpendicular to the plane of beat can flex more strongly than simple cilia and are capable of a greater tip velocity (Knight-Jones, 1954). These oral compound cilia probably help force food particles toward the mouth as they travel posteriorly along the food groove. Waller (1981) noted a postoral tuft in *O. edulis* which he described as rigid simple cilia, distinct from postoral cilia. He suggested the postoral tuft is sensory and may facilitate streaming of excess mucus and food posteriorly. Oral compound cilia described above are located between the postoral tuft and the mouth of *C. hastata*. Possibly these oral compound cilia serve a sensory function in selecting or rejecting food particles before they enter the mouth.

Luminal spaces within each primary gill filament also have been observed in *C. virginica* (Galtsoff, 1964; Elston, 1980) and *M. edulis* (Bayne, 1971). However, we were unable to observe any connection of these spaces to each other or with other vascular tissue. Elston (1980) noted that the spaces within the gill filaments—as well as other vascular tissues—may contain wandering amoeboid cells, suggesting a possible connection between luminal spaces. Prytherch (1934) observed blood cells circulating to the base of the gill filaments.

Structure of the larval eyespots in *C. hastata* is similar to that as described by Bayne (1971) for *M. edulis*, a cup-shaped group of small pigment granules deposited in a single cell. Galtsoff (1964) described the eyespots of *O. edulis* as consisting of several pigmented cells arranged in a circle around a transparent lens. Hickman and Gruffydd (1971) observed several pigment cells surrounding a lens, similar to Galtsoff, but noted that the granules were in the shape of a cup. There is little doubt that the eyespots are functional sensory organs in the larval stage; Galtsoff (1964) described nerve tracts leading to the eyespots of *O. edulis* and Bayne (1964) demon-

strated that the appearance of the eyespots coincided with a change in phototactic behavior in *M. edulis* larvae.

Bivalve larval development generally is considered to be similar among species. Superficially, pectinids show little variation in development. With the exception of *Equichlamys bifrons* (Dix, 1976), all species investigated have a small egg (60–80 μm) and a planktotrophic larval stage. Duration of larval development varies with temperature and diet, but generally larvae reared at 15–18°C metamorphose 20–35 days after fertilization. Yet, as recent studies on larval hinge morphology (Lutz *et al.*, 1982) have demonstrated, there are subtle differences between species, enough to make them distinguishable from each other. In this study we have noted several differences in the morphology of *C. hastata* to that reported in the literature. Of particular interest are the unique compound cilia situated at the mouth region, the presence of a ligament pit in larval valves, and the observation that the postoral band is comprised of simple cilia. Examination of other bivalve larvae may reveal other structures previously unrecorded and we may begin to appreciate subtle morphological differences in larvae that are otherwise superficially similar.

Acknowledgments

We thank Canadian Benthic Ltd. for providing adult *C. hastata* and the encouragement to pursue this study. This research was supported by a British Columbia Science Council Graduate Research, Engineering, and Technology Award and a Western Canadian Universities Marine Biological Station Graduate Award to CAH and a Natural Sciences and Engineering Research Council of Canada operating grant to RDB.

Literature Cited

Andrews, J. D. 1979. Pelecypoda: Ostreidae. Pp. 293–341 in *Reproduction of Marine Invertebrates,* Vol. 5, A. C. Giese and J. S. Pearse, eds. Plenum Press, New York.

Ansell, A. D. 1961. Reproduction, growth and mortality of *Venus striatula* (Da Costa) in James Bay, Millport. *J. Mar. Biol. Assoc. U.K.* **41:** 191–215.

Bayne, B. L. 1964. The responses of the larvae of *Mytilus edulis* L. to light and to gravity. *Oikos* **15:** 162–174.

Bayne, B. L. 1971. Some morphological changes that occur at the metamorphosis of the larvae of *Mytilus edulis.* Pp. 259–280 in *Proceedings of the Fourth European Marine Biology Symposium,* D. J. Crisp, ed. Cambridge University Press, Cambridge.

Bernard, F. R. 1983. Catalogue of the living bivalvia of the eastern Pacific Ocean: Bering Strait to Cape Horn. *Can. Spec. Publ. Fish. Aquat. Sci.* **61:** 102 pp.

Calloway, C. B., and R. D. Turner. 1978. New techniques for preparing shells of bivalve larvae for examination with the scanning electron microscope. *Bull. Am. Malacol. Union Inc.* Pp. 17–24.

Carriker, M. R., and R. E. Palmer. 1979. Ultrastructural morphogenesis of prodissoconch and early dissoconch valves of the oyster, *Crassostrea virginica. Proc. Nat. Shellfish. Assoc.* **69:** 103–128.

Cloney, R. A., and E. Florey. 1968. Ultrastructure of cephalopod chromatophore organs. *Z. Zellforsch. Mikrosk. Anat.* **89:** 250–280.

Cragg, S. M., and H. A. Nott. 1977. The ultrastructure of the statocysts in the pediveliger larvae of *Pecten maximus* (L.) (Bivalvia). *J. Exp. Mar. Biol. Ecol.* **27:** 23–36.

Cranfield, H. J. 1973a. A study of the morphology, ultrastructure, and histochemistry of the foot of the pediveliger of *Ostrea edulis. Mar. Biol.* **22:** 187–202.

Cranfield, H. J. 1973b. Observations on the function of the glands of the foot of the pediveliger of *Ostrea edulis* during settlement. *Mar. Biol.* **22:** 211–223.

Dietrich, H. F., and A. R. Fontaine. 1975. A decalcification method for ultrastructure of echinoderm tissues. *Stain Technol.* **50**(5): 351–353.

Dix, T. G. 1976. Larval development of the queen scallop, *Equichlamys bifrons. Aust. J. Mar. Freshw. Res.* **27:** 399–403.

Elston, R. 1980. Functional anatomy, histology and ultrastructure of the soft tissues of the larval American oyster, *Crassostrea virginica. Proc. Nat. Shellfish Assoc.* **70:** 65–93.

Erdmann, W. 1935. Über die Entewicklung und die Anatomie der 'ansatzriefen' Larve von *Ostrea edulis,* mit Bemerkungen uber die Lebensgeschichte der Auster. *Wiss. Meeresunters. Abt. Helgol. (N.S.)* **19**(6): 1–25.

Galtsoff, P. S. 1964. The American oyster *Crassostrea virginica* Gmelin. *U. S. Fish. Wild. Serv. Fish. Bull.* **64:** 1–480.

Grau, G. 1959. *Pectinidae of the Eastern Pacific.* Allan Hancock Foundation Pacific Series Vol. 23. Univ. Southern Cal. Press, Los Angeles. 308 pp.

Gruffydd, Ll. D., D. J. W. Lane, and A. R. Beaumont. 1975. The glands of the larval foot in *Pecten maximus* L. and possible homologues in other bivalves. *J. Mar. Biol. Assoc. U.K.* **55:** 463–476.

Hickman, R. W., and Ll. D. Gruffydd. 1971. The histology of the larvae of *Ostrea edulis* during metamorphosis. Pp. 281–294 in *Proceedings of the Fourth European Marine Biology Symposium,* D. J. Crisp, ed. Cambridge University Press, Cambridge.

Knight-Jones, E. W. 1954. Relations between metachronism and the direction of ciliary beat in Metazoa. *Q. J. Microsc. Sci.* **95**(4): 503–521.

Lane, D. J. W., and J. A. Nott. 1975. A study of the morphology, fine structure and histochemistry of the foot of the pediveliger of *Mytilus edulis* (L.) *J. Mar. Biol. Assoc. U.K.* **55:** 477–495.

LePennec, M. 1978. Genese de la coquille larvaire et post larvaire chez divers bivalves marins. Ph.D. dissertation, University of Brest, Brest, Cedex, France.

LePennec, M. 1980. The larval and post-larval hinge of some families of bivalve molluscs. *J. Mar. Biol. Assoc. U.K.* **60:** 601–617.

Luft, J. H. 1961. Improvement on epoxy resin embedding methods. *J. Biochem. Biophys. Cytol.* **9:** 409–414.

Lutz, R. A., and H. Hidu. 1979. Hinge morphogenesis in the shells of larval and early post-larval mussels (*Mytilus edulis* (L.) and *Modiolus modiolus* (L.)). *J. Mar. Biol. Assoc. U.K.* **59:** 111–121.

Lutz, R. A., R. Mann, J. G. Goodsell, and M. Castagna. 1982. Larval and early post-larval development of *Arctica islandica. J. Mar. Biol. Assoc. U.K.* **62:** 745–769.

Lutz, R. A., J. Goodsell, M. Castagna, S. Chipman, C. Newell, H. Hidu, R. Mann, D. Jablonski, V. Kennedy, S. Siddall, R. Goldberg, H. Beattie, C. Falmagne, A. Chestnut, and A. Partridge. 1982. Preliminary observations on the usefulness of hinge structures for identification of bivalve larvae. *J. Shellfish Res.* **2**(1): 65–70.

Millonig, G. 1961. Advantages of a phosphate buffer for OsO_4 solutions in fixation. *J. Appl. Physiol.* **32:** 1637–1645.

Prytherch, H. F. 1934. The role of copper in the settling, metamorphosis, and distribution of the American oyster, *Ostrea virginica*. *Ecol. Monogr.* **4:** 47–107.

Raven, C. P. 1958. *Morphogenesis: the Analysis of Molluscan Development.* Pergamon Press, New York.

Richardson, K. C., L. Jarett, and E. H. Finke. 1960. Embedding in epoxy resins for ultrathin sectioning in electron microscopy. *Stain Technol.* **35:** 313–323.

Rubenstein, D. I., and M. A. R. Koehl. 1977. The mechanisms of filter feeding: some theoretical considerations. *Am. Nat.* **111:** 981–994.

Sastry, A. N. 1979. Pelecypoda. Pp. 113–292 in *Reproduction of Marine Invertebrates,* Vol. 5, A. C. Giese and J. S. Pearse, eds. Academic Press, New York.

Stenzel, H. B. 1964. Oysters. Composition of the larval shell. *Science* **145:** 155–156.

Strathmann, R. R., and E. Leise. 1979. On feeding mechanisms and clearance rates of molluscan veligers. *Biol. Bull.* **157:** 524–535.

Strathmann, R. R., T. L. Jahn, and J. R. C. Fonseca. 1972. Suspension feeding by marine invertebrate larvae: clearance of particles by ciliated bands of a rotifer, pluteus, and trochopore. *Biol. Bull.* **142:** 505–519.

Taylor, J. D., W. J. Kennedy, and A. Hall. 1969. The shell structure and mineralogy of the bivalvia. Introduction. Nuculacea—Trigonacea. *Bull. Br. Mus. (Nat. Hist.) Zool. Suppl.* **3:** 1–125.

Verdonk, N. H., and J. A. M. van den Biggelaar. 1983. Early development of the germ layers. Pp. 91–122 in *The Mollusca,* Vol. 3, *Development,* N. H. Verdonk, J. A. M. van den Biggelaar, and A. S. Tompa, eds. Academic Press, New York.

Verdonk, N. H., J. A. M. van den Biggelaar, and A. S. Tompa. 1983. *The Mollusca.* Vol. **3:** *Development.* Academic Press, New York. 352 pp.

Vogel, S. 1981. *Life in Marine Fluids.* Willard Grant Press, Boston.

Wada, S. K. 1968. Mollusca. Pp. 485–525 in *Invertebrate Embryology,* M. Kume and D. Dan, eds. (J. Dan, Engl. transl.) Publ. for U. S. Natl. Libr. Med., Wash. D. C. by Notlit Publ. House, Belgrade.

Waller, T. R. 1981. Functional morphology and development of veliger larvae of the European oyster, *Ostrea edulis* Linne. *Smithson. Contrib. Zool.* **328:** 70 pp.

Yonge, C. M. 1926. Structure and physiology of the organs of feeding and digestion in *Ostrea edulis*. *J. Mar. Biol. Assoc. U.K.* **14:** 295–386.